Available online at www.sciencedirect.com
ScienceDirect
Journal of Sound and Vibration 311 (2008) 297–313
JOURNAL OF SOUND AND VIBRATION
www.elsevier.com/locate/jsvi

Nonlinear modes of snap-through motions of a shallow arch

I. Breslavsky[a], K.V. Avramov[a,b,*], Yu. Mikhlin[c], R. Kochurov[a]

[a]Department of Gas and Fluid Mechanics, National Technical University "KhPI", Frunze St. 21, Kharkov 61002, Ukraine
[b]Department of Nonstationary Vibrations, A.N. Podgornogo Institute for Problems of Engineering Mechanical NAS of Ukraine, Dm. Pogarski St. 2/10, Kharkov 61046, Ukraine
[c]Department of Applied Mathematics, National Technical University "KhPI", Frunze St. 21, Kharkov 61002, Ukraine

Received 17 February 2007; received in revised form 30 August 2007; accepted 11 September 2007
Available online 26 October 2007

Abstract

Nonlinear modes of snap-through motions of a shallow arch are analyzed. Dynamics of shallow arch is modeled by a two-degree-of-freedom system. Two nonlinear modes of this discrete system are treated. The methods of Ince algebraization and Hill determinants are used to study stability of nonlinear modes. The analytical results are compared with the data of the numerical simulations.

1. Introduction

The shallow arches are used in civil, mechanical and aerospace engineering as parts of complex structures. Arches are used in electromechanical equipments to switch between several equilibrium positions. Moreover, the shallow aches can be used for vibration isolation [1] and for vibrations absorption [2–4].

Many researches are studied static and dynamics of the shallow arches. Timoshenko [5] considered the simply supported sinusoidal arch under the action of a uniformly distributed load. He determined the lateral static load, which leads to the snap-through motions of shallow arch. Dinnik and Grigoluk [6,7] obtained that snap-through motions consist of both symmetric and asymmetric simply supported beams modes. Fung and Kaplan [8] generalized the results of static analysis of shallow arches to the case of arbitrary lateral loads including concentrated forces.

One of the first efforts to analyze the snap-through motions of shallow arch was presented in the papers [9,10]. In particular, the sufficient conditions of stability and instability of shallow arches under the action of static loads were considered in Ref. [9]. Asymmetric snap-through motions of shallow arches under the action of high-frequency periodic force were considered by Hung [11]. In this paper, the snap-through vibrations were split into the fast and slow motions. The asymptotic procedure for analysis of snap-through motions of shallow arches was suggested in the book [12]. Lenci and Tarantino [13] were used the Melnikov function to study the chaotic snap-through motions of shallow arches. The arch under the action of the transverse

*Corresponding author. Department of Nonstationary Vibrations, A.N. Podgornogo Institute for Problems of Engineering Mechanical NAS of Ukraine, Dm. Pogarski St. 2/10, Kharkov 61046, Ukraine. Tel.: +38 057 7322505.
E-mail address: kvavr@kharkov.ua (K.V. Avramov).

0022-460X/$ - see front matter © 2007 Elsevier Ltd. All rights reserved.
doi:10.1016/j.jsv.2007.09.015

distributed force is considered in the paper [14]. Moreover, the lateral load with prescribed end motion with constant speed acts additionally on this arch. The snap-through motions of the arch with different velocities of lateral forces were considered. The arch with one end pinned and the other end attached to a mass is considered in the paper [15]. The simply supported arch under the action of moving load with constant velocity is considered in the paper [16].

In the present paper, the nonsymmetrical snap-through motions of the shallow arch are considered. Two-degree-of-freedom nonlinear model is derived to study these motions. The nonlinear vibrations modes of the snap-through truss are considered. One of these modes corresponds to the symmetrical snap-through motions of the shallow arch and the other mode corresponds to the nonsymmetrical snap-through motions. The Ince algebraization and the method of Hill determinants are used to study stability of the snap-through motions.

2. The problem formulation

Motions of the shallow arch (Fig. 1) are considered in this paper. The equation of arch motions is the following [9–11]:

$$\frac{EA}{2L}y_{xx}\int_0^L\left\{\left(\frac{\partial y_0}{\partial x}\right)^2-\left(\frac{\partial y}{\partial x}\right)^2\right\}\mathrm{d}x+EI(y-y_0)_{xxxx}+\rho A y_{tt}=0, \tag{1}$$

where $y(x,t)$ is a dynamic flexure of the arch; $y_0(x)$ is an initial flexure of the arch; A and I are the area and moment of inertia of a cross section; E and ρ are the Young's modulus and material density of the arch; L is a length of the arch. The initial flexure of the arch has the following form:

$$y_0=\lambda_1\sin\left(\frac{\pi x}{L}\right).$$

The dimensionless variables are introduced in the following form:

$$u_0=\frac{y_0}{\lambda_1},\quad u=\frac{y}{\lambda_1},\quad \xi=\frac{\pi}{L}x,\quad \tau=\left(\frac{\pi}{L}\right)^2\sqrt{\frac{E}{\rho}}\lambda_1 t. \tag{2}$$

Thin arches are considered in this paper, so these arches satisfy the following condition:

$$\varepsilon=\frac{r^2}{\lambda_1^2}\ll 1, \tag{3}$$

where r is a radius gyration of cross-section. Now the equation of motions in dimensionless form can be written as

$$\frac{u_{\xi\xi}}{2\pi}\int_0^\pi(u_{0,\xi}^2-u_\xi^2)\,\mathrm{d}\xi+\varepsilon(u-u_0)_{\xi\xi\xi\xi}+u_{\tau\tau}=0, \tag{4}$$

where

$$u_0=\sin(\xi). \tag{5}$$

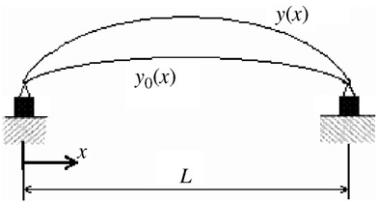

Fig. 1. The shallow arch.

The dimensionless flexure of the arch is presented in the form

$$u = \sin(\xi) + \sum_{i=1} \eta_i(\tau)\sin(i\xi), \tag{6}$$

where η_1, η_2,... are generalized coordinates. Then expressions (5) and (6) are substituted into Eq. (4) and the separation of variables is carried out. As a result, the following dynamical system is derived:

$$\begin{aligned} \ddot{\eta}_1 + \varepsilon\eta_1 &= (1+\eta_1)\chi(\eta_1,\eta_2,\ldots), \\ \ddot{\eta}_i + \varepsilon i^4\eta_i &= i^2\eta_i\chi(\eta_1,\eta_2,\ldots), \quad i = 2,3,\ldots, \\ \chi(\eta_1,\eta_2,\ldots) &= -0.5\left(\eta_1 + 0.5\sum_{i=1}^{n}\eta_i^2 i^2\right). \end{aligned} \tag{7}$$

Only two vibration modes as shown in Eq. (6) are taken into account in the future analysis: $\eta_3 = \eta_4 = \cdots = 0$. The following new variables are introduced: $\theta_1 = 1+\eta_1$, $\theta_2 = \eta_2$. Then the equations of motion have the following form:

$$\begin{aligned} \ddot{\theta}_1 + \varepsilon(\theta_1 - 1) &= \theta_1\chi(\theta_1,\theta_2), \\ \ddot{\theta}_2 + 16\varepsilon\theta_2 &= 4\theta_2\chi(\theta_1,\theta_2), \\ \chi(\theta_1,\theta_2) &= -0.5(0.5(\theta_1^2 - 1) + 2\theta_2^2). \end{aligned} \tag{8}$$

The equilibriums of the dynamical system (8) are considered. The symmetric static flexure ($\theta_2 = 0$; $\theta_1 \neq 0$) is analyzed. This flexure corresponds to the exact solution of the second equation of system (8). Then the equilibriums are defined from the cubic equations

$$\varepsilon(\theta_1 - 1) = -\theta_1\tfrac{1}{4}(\theta_1^2 - 1). \tag{9}$$

If

$$\varepsilon < \tfrac{1}{16}, \tag{10}$$

then three equilibriums exist in dynamical system (8). These fixed points are defined in the following form:

$$\theta_1^{(1)} = 1, \quad \theta_1^{(2)} = \frac{-1+\sqrt{1-16\varepsilon}}{2}, \quad \theta_1^{(3)} = \frac{-1-\sqrt{1-16\varepsilon}}{2}. \tag{11}$$

At $\varepsilon = 1/16$ the saddle-node bifurcation of the equilibriums take place in the dynamical system Eq. (8). In this point the equilibriums $\theta_1^{(2)}$ and $\theta_1^{(3)}$ are merged. If $\varepsilon > 1/16$, only one equilibriums $\theta_1^{(1)} = 1$ exists.

3. Nonlinear normal modes (NNMs)

NNMs are a nonlinear extension of the normal modes of linear systems. NNM of undamped discrete system is a synchronous periodic vibration where all material points of the system reach their extreme values simultaneously. When a discrete system vibrates in a NNM, the oscillations are presented by a line in its configuration space. This line is termed a "modal line".

The NNM $\theta_2 = 0$ always exists in system (8). The NNM $\theta_1 = 0$ exists in the unperturbated system (8) ($\varepsilon = 0$). At $\varepsilon \neq 0$ this NNM can be presented as

$$\theta_1 = \theta_1(\theta_2) = \varepsilon g(\theta_2). \tag{12}$$

So, θ_2 are a new independent variable. The standard procedure from Refs. [12,17] is used to derive the differential equation of the NNMs in the system configuration space. The following relation is used:

$$\ddot{\theta}_1(\tau) = \theta_1''(\theta_2)\dot{\theta}_2^2(\tau) + \theta_1'(\theta_2)\ddot{\theta}_2(\tau), \tag{13}$$

where the prime denotes a differentiation with respect to θ_2. The following energy integral exists in system (8):

$$0.5(\dot{\theta}_1^2 + \dot{\theta}_2^2) + \Pi = h, \tag{14}$$

$$\Pi = \Pi_0 + \varepsilon\Pi_1 = \tfrac{1}{2}\theta_1^2\theta_2^2 + \tfrac{1}{16}\theta_1^4 - \tfrac{1}{8}\theta_1^2 - \tfrac{1}{2}\theta_2^2 + \theta_2^4 + \varepsilon\left(\tfrac{1}{2}\theta_1^2 - \theta_1 + 8\theta_2^2\right),$$

where Π is a potential energy of the system; $0.5(\dot{\theta}_1^2 + \dot{\theta}_2^2)$ is a kinetic energy of the system; h is a value of the system energy. The following expression is derived from Eq. (14):

$$\dot{\theta}_2^2(\tau) = \frac{2(h-\Pi)}{1+\theta_1'^2(\theta_2)}. \tag{15}$$

Now relations (13) and (15) are substituted into the first equation of system (8). Taking into account the first Eq. (8), the differential equation for the NNMs trajectories in configuration space is derived:

$$\theta_1'' \frac{2(h-\Pi)}{1+\theta_1'^2} - \theta_1' \frac{\partial \Pi}{\partial \theta_2} = -\frac{\partial \Pi}{\partial \theta_1}. \tag{16}$$

Note, that Eq. (16) has singular points at the maximum isoenergetic surface

$$\Pi(\theta_{2,\max}) = h \tag{17}$$

where $\theta_{2,\max}$ is the vibration amplitude. Eq. (16) must be completed by the following boundary conditions:

$$\left[\theta_1' \frac{\partial \Pi}{\partial \theta_2}\right]_{\theta_2=\theta_{2,\max}} = \left.\frac{\partial \Pi}{\partial \theta_1}\right|_{\theta_2=\theta_{2,\max}}. \tag{18}$$

Eq. (18) is the condition of orthogonality of the NNM trajectory to the maximum isoenergetic surface. Therefore, this trajectory can be analytically continued to the maximum isoenergetic surface [12,17].

Now Eq. (12) is substituted into Eq. (16) and the terms $O(\varepsilon)$ are collected. As a result the following equation is derived:

$$g''2(h - \Pi_0|_{\theta_1=\varepsilon g}) + g'(4\theta_2^3 - \theta_2) - 1 - 0.25g + g\theta_2^2 = 0. \tag{19}$$

Taking into account relation (14), Eq. (17) is rewritten as

$$\Pi_0(\theta_{2,\max}) = h. \tag{20}$$

This equation is presented as

$$\theta_{2,\max}^4 - \tfrac{1}{2}\theta_{2,\max}^2 = h. \tag{21}$$

The terms $O(\varepsilon)$ in the boundary conditions (18) have the following form:

$$g'(\theta_{2,\max})(4\theta_{2,\max}^3 - \theta_{2,\max}) - 1 - 0.25g(\theta_{2,\max}) + g(\theta_{2,\max})\theta_{2,\max}^2 = 0. \tag{22}$$

The function $g(\theta_2)$ is presented in the form of power series:

$$g(\theta_2) = \sum_{i=0}^{\infty} b_i \theta_2^i. \tag{23}$$

Series (23) is substituted into Eq. (19) and terms of the same degree of θ_2 are equated. As a result the system of linear algebraic equations with respect to b_i is derived. If series (23) is substituted into Eq. (22), the additional linear algebraic equation is derived. Thus, the system of linear algebraic equations with respect to $(b_0, b_1, \ldots)$ is obtained. The solution of this system is the following:

$$\begin{aligned}
&b_{2j-1} = 0; j = 1, 2, \ldots,\\
&b_0 = \frac{\beta_0 + \beta_2\theta_{2,\max}^2 + \beta_4\theta_{2,\max}^4 + \beta_6\theta_{2,\max}^6 + \beta_8\theta_{2,\max}^8 + \beta_{10}\theta_{2,\max}^{10} + \beta_{12}\theta_{2,\max}^{12}}{\alpha_0 + \alpha_2\theta_{2,\max}^2 + \alpha_4\theta_{2,\max}^4 + \alpha_6\theta_{2,\max}^6 + \alpha_8\theta_{2,\max}^8 + \alpha_{10}\theta_{2,\max}^{10} + \alpha_{12}\theta_{2,\max}^{12} + \alpha_{14}\theta_{2,\max}^{14}},\\
&b_2 = \frac{\gamma_0 + \gamma_2\theta_{2,\max}^2 + \gamma_4\theta_{2,\max}^4 + \gamma_6\theta_{2,\max}^6 + \gamma_8\theta_{2,\max}^8 + \gamma_{10}\theta_{2,\max}^{10}}{\alpha_0 + \alpha_2\theta_{2,\max}^2 + \alpha_4\theta_{2,\max}^4 + \alpha_6\theta_{2,\max}^6 + \alpha_8\theta_{2,\max}^8 + \alpha_{10}\theta_{2,\max}^{10} + \alpha_{12}\theta_{2,\max}^{12} + \alpha_{14}\theta_{2,\max}^{14}},\\
&b_4 = \frac{\delta_0 + \delta_2\theta_{2,\max}^2 + \delta_4\theta_{2,\max}^4}{\chi_0 + \chi_2\theta_{2,\max}^2 + \chi_4\theta_{2,\max}^4 + \chi_6\theta_{2,\max}^6 + \chi_8\theta_{2,\max}^8 + \chi_{10}\theta_{2,\max}^{10}},
\end{aligned} \tag{24}$$

where

$$\alpha_0 = -0.2197, \alpha_2 = 1.1133, \alpha_4 = 13.8594, \alpha_6 = -133.938,$$
$$\alpha_8 = 489.5, \alpha_{10} = -1018, \alpha_{12} = 1184, \alpha_{14} = -640,$$
$$\beta_0 = 0.8789, \beta_2 = -2.5781, \beta_4 = -70.6875, \beta_6 = 462.75, \beta_8 = -1242,$$
$$\beta_{10} = 1872, \beta_{12} = -1152,$$
$$\gamma_0 = 0.2344, \gamma_2 = -1.4375, \gamma_4 = -12, \gamma_6 = 65.5, \gamma_8 = -144, \gamma_{10} = 160;$$
$$\delta_0 = 0.25, \delta_2 = -1.25, \delta_4 = 12,$$
$$\chi_0 = -0.2344, \chi_2 = 0.6875, \chi_4 = 17.25, \chi_6 = -109, \chi_8 = -0.2344, \chi_{10} = -160.$$

The numerical calculations show, that the terms $b_6\theta_2^6, b_8\theta_2^8, \ldots$ are essentially less than the terms of the smaller degrees. Therefore, in the future numerical analysis only the first three terms of the expansion (23) are taken into account.

Now the motions in time on the modal line (23) and (24) are determined. The NNM (12) is substituted into the second equation of system (8). As a result the following ODE is derived:

$$\ddot{\theta}_2 + 16\varepsilon\theta_2 + \varepsilon^2\theta_2 g^2(\theta_2) - \theta_2 + 4\theta_2^3 = 0. \tag{25}$$

The equilibriums of system (8) ($\theta_1 \neq 0$; $\theta_2 = 0$) are treated in Section 2. Here the equilibriums of Eq. (25), which differ from the equilibriums ($\theta_1 \neq 0$; $\theta_2 = 0$), are considered. The equilibriums of system (25) can be determined from the following cubic equation:

$$16\varepsilon\theta_2 = 4\theta_2\left[\tfrac{1}{4}(1 - O(\varepsilon^2)) - \theta_2^2\right]. \tag{26}$$

Eq. (26) has the following roots:

$$\theta_2^{(1)} = 0; \theta_2^{(2,3)} = \pm\frac{\sqrt{1 - 16\varepsilon - O(\varepsilon^2)}}{2}.$$

Thus, three equilibriums exist at $\varepsilon < 1/16$. This inequality coincides with Eq. (10).

The harmonic balance method is used to study the periodic solutions of system (25). These periodic motions are taken in the form

$$\theta_2(\tau) = \theta_{2,\max}\cos(\omega\tau). \tag{27}$$

Solution (27) is substituted into Eq. (25). As a result, the equation for the frequency of the oscillations is derived:

$$\omega^2 = 16\varepsilon + \varepsilon^2(b_0^2 + b_0 b_2\theta_{2,\max}^4 + 0.375(b_2^2 + 2b_0 b_4)\theta_{2,\max}^4 + 0.625 b_2 b_4\theta_{2,\max}^6) - 1 + 3\theta_{2,\max}^2. \tag{28}$$

The backbone curves are calculated by Eq. (28). These curves are shown in Fig. 2. Fig. 2a,b corresponds to the values $\varepsilon = 0.01$ and 0.05, respectively. The stable and unstable vibrations are shown by solid and dotted lines, respectively. Stability analysis of these vibrations is presented in Section 4.

The direct numerical integration of system (8) is carried out to estimate the accuracy of the above-derived NNM. For this integration the initial conditions, corresponding to the NNM (12), are taken in the following form:

$$\dot{\theta}_1(0) = \dot{\theta}_2(0) = 0; \theta_2(0) = \theta_{2,\max}; \theta_1(0) = \varepsilon g(\theta_{2,\max}).$$

Fig. 3 shows the results of the numerical simulations of the NNM trajectories in the system configuration space. These trajectories correspond to the stable NNM and were obtained for the parameters: (a)$-\varepsilon = 0.06$; $h = 14$; (b)$-\varepsilon = 0.03$; $h = 1.35$; (c)$-\varepsilon = 0.03$; $h = 2.86$.

The direct numerical simulations of the dynamical system (8) are carried out in a case of unstable NNM too. Fig. 4 shows results of these calculations in the system configuration space at $\varepsilon = 0.06$; $h = 0.09$. Obviously, almost periodic snap-through motions take place when the NNM is unstable. The red lines in Figs. 3 and 4 show the nonlinear modes, which are obtained analytically. Eqs. (12), (23), and (24) are used to calculate the red lines.

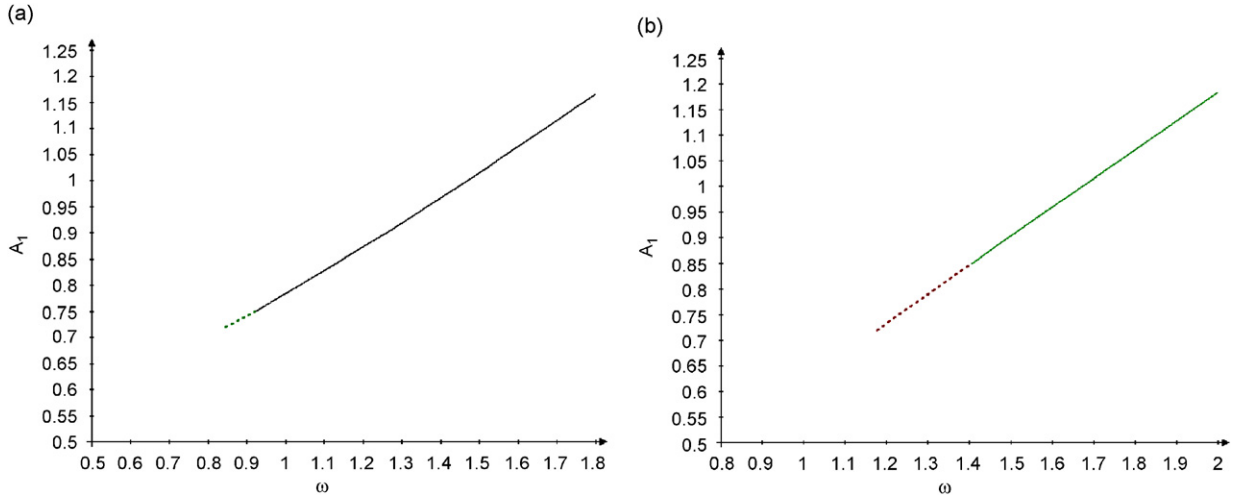

Fig. 2. The backbone curves of the nonlinear mode (12), (23), and (24): (a) $\varepsilon = 0.01$ and (b) $\varepsilon = 0.05$.

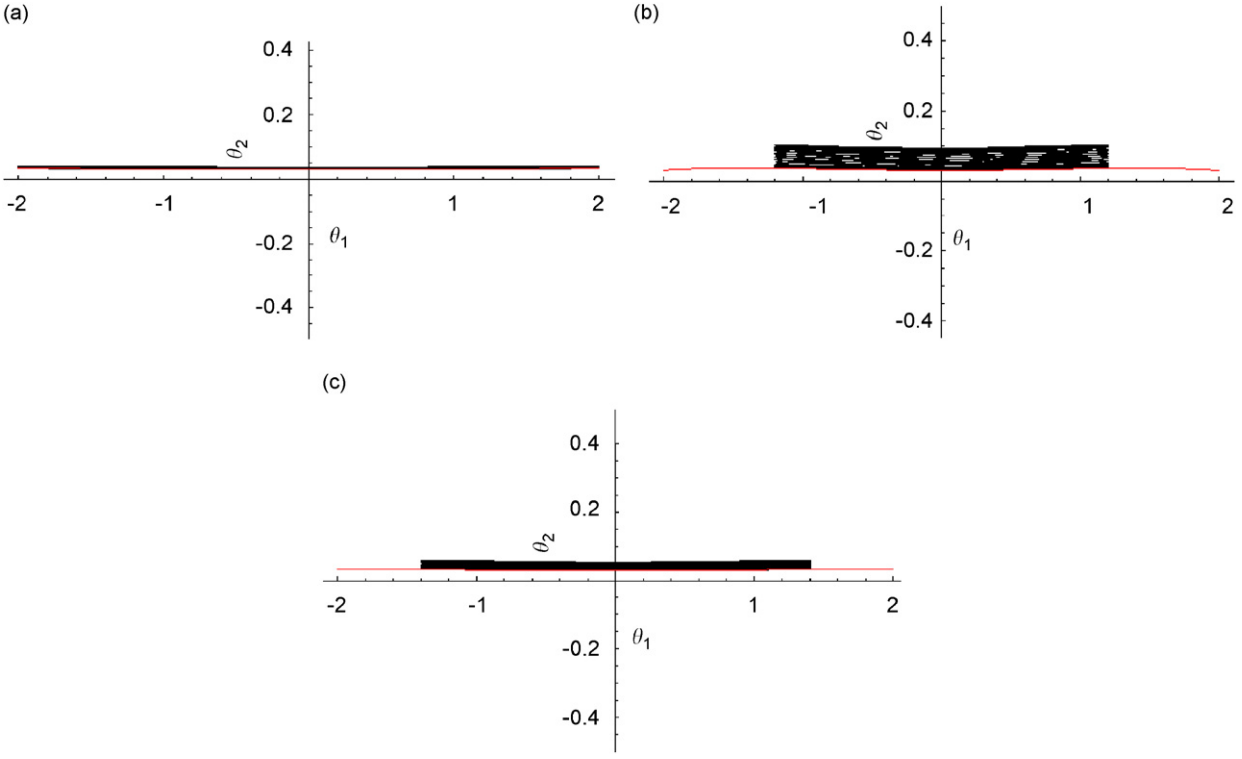

Fig. 3. Results of direct numerical simulation of the nonlinear mode (12), (23), and (24). The trajectories correspond to the following parameters: (a) $\varepsilon = 0.06$, $h = 14$; (b) $\varepsilon = 0.03$, $h = 1.35$; (c) $\varepsilon = 0.03$, $h = 2.86$.

Now the motions on the second NNM $\theta_2 = 0$ are analyzed. The relation $\theta_2 = 0$ is substituted into the first equation of system (8). The harmonic balance method is used to study vibrations in the obtained equation. These vibrations are presented in the following form:

$$\theta_1(\tau) = B_0 + B_1 \cos(\omega\tau) + B_2 \cos(2\omega\tau). \tag{29}$$

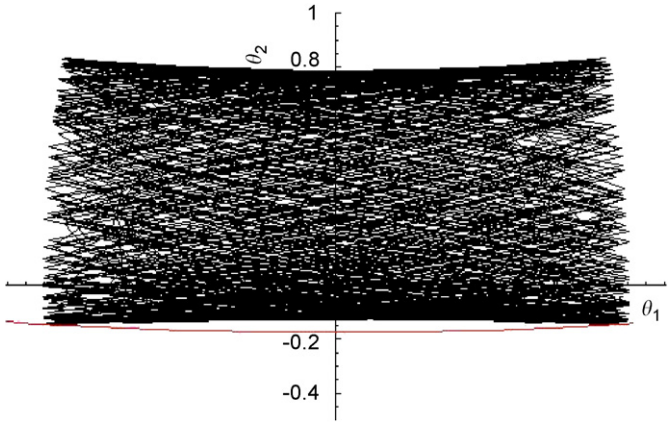

Fig. 4. Results of direct numerical simulation of the unstable NNM (12), (23) and (24).

Following the harmonic balance method, the parameters B_0, B_1, B_2 are determined from the next system of nonlinear algebraic equations:

$$\begin{aligned}
&4(\varepsilon B_0-\varepsilon)+B_0^3+1.5B_0B_1^2+0.75B_1^2B_2+1.5B_0B_2^2+1.5B_1B_2^2-B_0=0,\\
&-3\varepsilon B_2+0.75B_2-2.25B_0^2B_2-0.375B_1^2B_2-3B_0B_2^2+0.375B_0B_1^2+0.1875B_2^3=0,\\
&-\omega^2B_1+\varepsilon B_1+0.75B_1B_0^2+0.1875B_1^3+0.75B_0B_1B_2-0.25B_1=0.
\end{aligned} \tag{30}$$

System (30) is used to calculate the backbone curves. Fig. 5 shows results of these calculations. Fig. 5a,b corresponds to $\varepsilon=0.01$ and 0.05, respectively. The stable and unstable vibrations are shown by solid and dotted lines, respectively. The stability analysis of these vibrations is presented in the next section.

4. Stability of NNM

It is assumed, that the periodic motions $\tilde{\theta}_1(\tau),\tilde{\theta}_2(\tau)$ take place in the dynamical system (8). The small perturbations u, v from the periodic motions, which are determined by the equations $\theta_1=\tilde{\theta}_1(\tau)+u;\theta_2=\tilde{\theta}_2(\tau)+v$, are considered. These perturbations satisfy the following ODEs:

$$\ddot{u}+\varepsilon u+\tfrac{3}{4}u\tilde{\theta}_1^2+2v\tilde{\theta}_1\tilde{\theta}_2-\tfrac{1}{4}u+u\tilde{\theta}_2^2=0, \tag{31a}$$

$$\ddot{v}+16\varepsilon v+12v\tilde{\theta}_2^2+2u\tilde{\theta}_1\tilde{\theta}_2-v+v\tilde{\theta}_1^2=0. \tag{31b}$$

Now the stability of the NNM $\theta_2=0$ is investigated. Then the system of variational equations can be written as

$$\ddot{u}+\varepsilon u+\tfrac{3}{4}u\tilde{\theta}_1^2-\tfrac{1}{4}u=0, \tag{32a}$$

$$\ddot{v}+16\varepsilon v-v+v\tilde{\theta}_1^2=0. \tag{32b}$$

Note, that the variables u, v define the perturbations along the NNM and in the orthogonal direction, respectively. We remind, that the considered system (8) is conservative. The periodic motions of such system are unstable in the sense of Lyapunov, but such motions are orbital stable [2,17]. Therefore, in this paper orbital stability of the NNM is studied. Motions along the NNM are not affected on the orbital stability [2]. Therefore, only the small perturbations in the orthogonal directions, which are described by Eq. (32b), must be considered. The Ince algebraization [18–20] is used to study stability of the NNM. The variable $x=\tilde{\theta}_1(\tau)$ is chosen as new independent variable instead of τ. In this case a presentation of the solutions in time is not used. This is the advantage of such an approach.

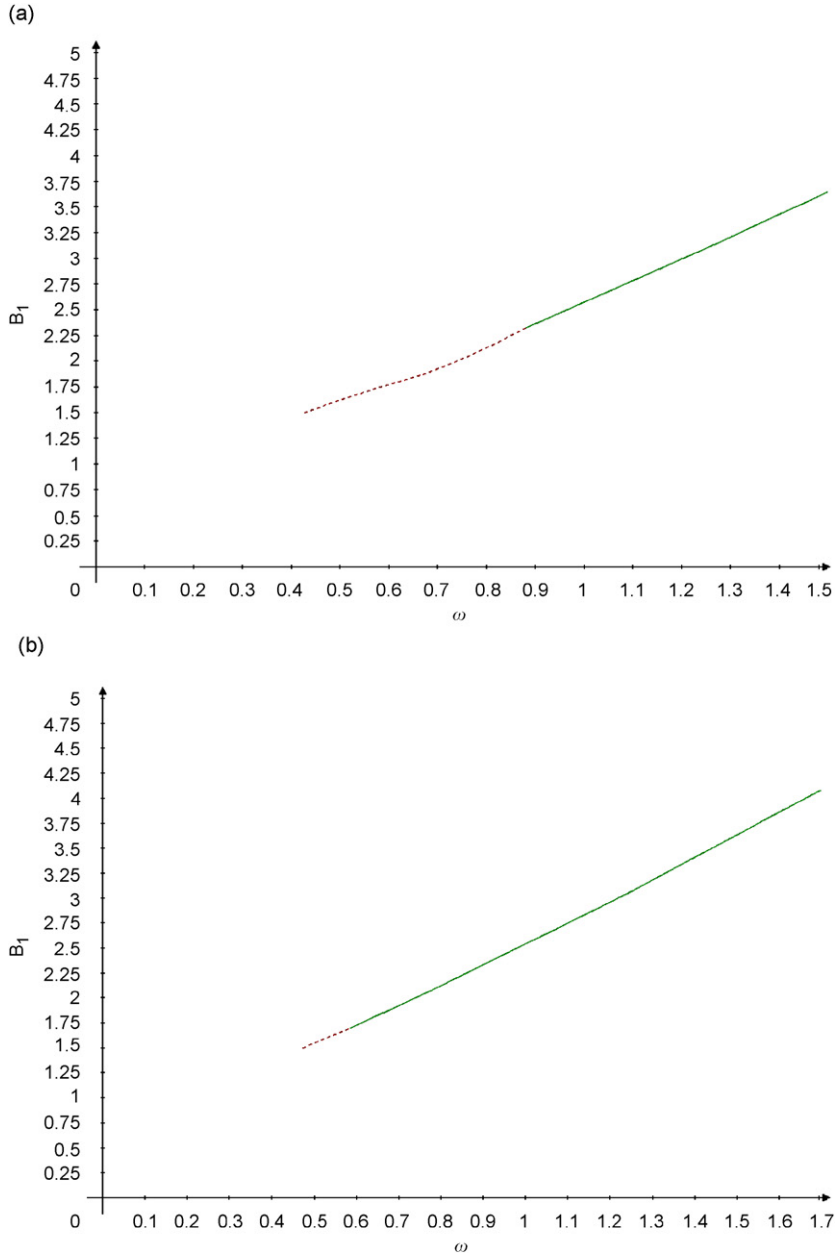

Fig. 5. The backbone curves of nonlinear mode (29): (a) $\varepsilon = 0.01$ and (b) $\varepsilon = 0.05$.

As follows from system (8), the variable x satisfy the equation

$$\ddot{x} = -\varepsilon(x-1) - \tfrac{1}{4}x^3 + \tfrac{1}{4}x. \tag{33}$$

Then, the following equation, which follows from the energy integral, is true:

$$\dot{x}^2 = 2(h - \Pi|_{\theta_2=0}), \tag{34}$$

$$\Pi|_{\theta_2=0} = \tfrac{1}{16}\theta_1^4 - \tfrac{1}{8}\theta_1^2 + \varepsilon\left(\tfrac{1}{2}\theta_1^2 - \theta_1\right).$$

Taking into account $\ddot{v} = v''\dot{x}^2 + v'\ddot{x}$, the variational Eq. (32b) is rewritten in the following form:

$$2v''(x)(h - \Pi_{\theta_2=0}) + v'(x)\ddot{x} + 16\varepsilon v(x) - v(x) + v(x)x^2 = 0, \tag{35}$$

where prime denotes a differentiation with respect to the new independent variable. Note, that the indexes of singular points of Eq. (35) are the following [18,19]: $\alpha_1 = 0$ and $\alpha_2 = 1/2$. It is shown in Ref. [18], that the solutions on the boundaries of stable/unstable regions are determined as

$$v_1 = \sum_{i=0}^{\infty} \alpha_i x^i, \tag{36a}$$

$$v_2 = \sqrt{(X_1 - x)(x - X_2)} \sum_{i=0}^{\infty} \beta_i x^i, \tag{36b}$$

$$v_3 = \sqrt{x - X_2} \sum_{i=0}^{\infty} \gamma_i x^i, \tag{36c}$$

$$v_4 = \sqrt{X_1 - x} \sum_{i=0}^{\infty} \delta_i x^i, \tag{36d}$$

where X_1, X_2 are amplitudes of vibrations, which are determined from the equation:

$$\Pi_{\theta_2=0} = h. \tag{37}$$

The solutions v_1, v_2, v_3, and v_4 in Eqs. (36a)–(36d) are substituted into Eq. (35). As a result, four nonlinear algebraic equations with respect to x are derived:

$$2\sum_{i=2}^{\infty} i(i-1)\alpha_i x^{i-2}\left(h - \frac{1}{16}x^4 + \frac{1}{8}x^2 - \varepsilon\left(\frac{1}{2}x^2 - x\right)\right) + \sum_{i=1}^{\infty} i\alpha_i x^{i-1}\left(-\varepsilon(x-1) - \frac{1}{4}x^3 + \frac{1}{4}x\right) + (16\varepsilon - 1 + x^2)\sum_{i=0}^{\infty}\alpha_i x^i = 0, \tag{38a}$$

$$2\left(-\frac{(X_1 - X_2)^2}{4}\sum_{i=0}^{\infty}\beta_i x^i - (2x - X_1 - X_2)(X_1 - x)(x - X_2)\sum_{i=1}^{\infty} i\beta_i x^{i-1} + (X_1 - x)^2(x - X_2)^2\sum_{i=2}^{\infty} i(i-1)\beta_i x^{i-2}\right)\left(h - \frac{1}{16}x^4 + \frac{1}{8}x^2 - \varepsilon\left(\frac{1}{2}x^2 - x\right)\right) + \left(-\frac{1}{2}(2x - X_1 - X_2)(X_1 - x)(x - X_2)\sum_{i=0}^{\infty}\beta_i x^i + (X_1 - x)^2(x - X_2)^2\sum_{i=1}^{\infty} i\beta_i x^{i-1}\right) \times \left(-\varepsilon(x-1) - \frac{1}{4}x^3 + \frac{1}{4}x\right) + (16\varepsilon - 1 + x^2)(X_1 - x)^2(x - X_2)^2\sum_{i=0}^{\infty}\beta_i x^i = 0, \tag{38b}$$

$$2\left(-\frac{1}{4}\sum_{i=0}^{\infty}\gamma_i x^i + (x - X_2)\sum_{i=1}^{\infty} i\gamma_i x^{i-1} + (x - X_2)^2\sum_{i=2}^{\infty} i(i-1)\gamma_i x^{i-2}\right)\left(h - \frac{1}{16}x^4 + \frac{1}{8}x^2 - \varepsilon\left(\frac{1}{2}x^2 - x\right)\right) + \left(\frac{1}{2}(x - X_2)\sum_{i=0}^{\infty}\gamma_i x^i + (x - X_2)^2\sum_{i=1}^{\infty} i\gamma_i x^{i-1}\right)\left(-\varepsilon(x-1) - \frac{1}{4}x^3 + \frac{1}{4}x\right) + (16\varepsilon - 1 + x^2)(x - X_2)^2\sum_{i=0}^{\infty}\gamma_i x^i = 0, \tag{38c}$$

$$2\left(-\frac{1}{4}\sum_{i=0}^{\infty}\delta_i x^i+(x-X_1)\sum_{i=1}^{\infty}i\delta_i x^{i-1}+(x-X_1)^2\sum_{i=2}^{\infty}i(i-1)\delta_i x^{i-2}\right)\left(h-\frac{1}{16}x^4+\frac{1}{8}x^2-\varepsilon\left(\frac{1}{2}x^2-x\right)\right)$$
$$+\left(\frac{1}{2}(x-X_1)\sum_{i=0}^{\infty}\delta_i x^i+(x-X_1)^2\sum_{i=1}^{\infty}i\delta_i x^{i-1}\right)\left(-\varepsilon(x-1)-\frac{1}{4}x^3+\frac{1}{4}x\right)$$
$$+(16\varepsilon-1+x^2)(x-X_1)^2\sum_{i=0}^{\infty}\delta_i x^i=0. \tag{38d}$$

Equating the coefficients at the same degrees of x, four independent systems of homogeneous linear algebraic equations are derived from Eqs. (38a)–(38d). These systems have nontrivial solutions, if their determinants are equal to zero. Every of these determinants give the boundaries between stable and unstable vibrations on the parametric plane (h, ε).

Fig. 6 shows the boundary between stable/unstable oscillations. Region of the unstable oscillations is shaded. Numerical calculations of the boundaries of unstable vibrations are carried out using the determinants of the different orders. These calculations show, that the determinants of the six order are enough for reliable results. As an example, the determinant of the six order, which is derived from the solution v_2, is presented in Appendix A.

The boundary between stable and unstable vibrations (Fig. 6) is checked by calculations of the fundamental matrixes and the multipliers [21]. The obtained results confirm the above-presented analysis.

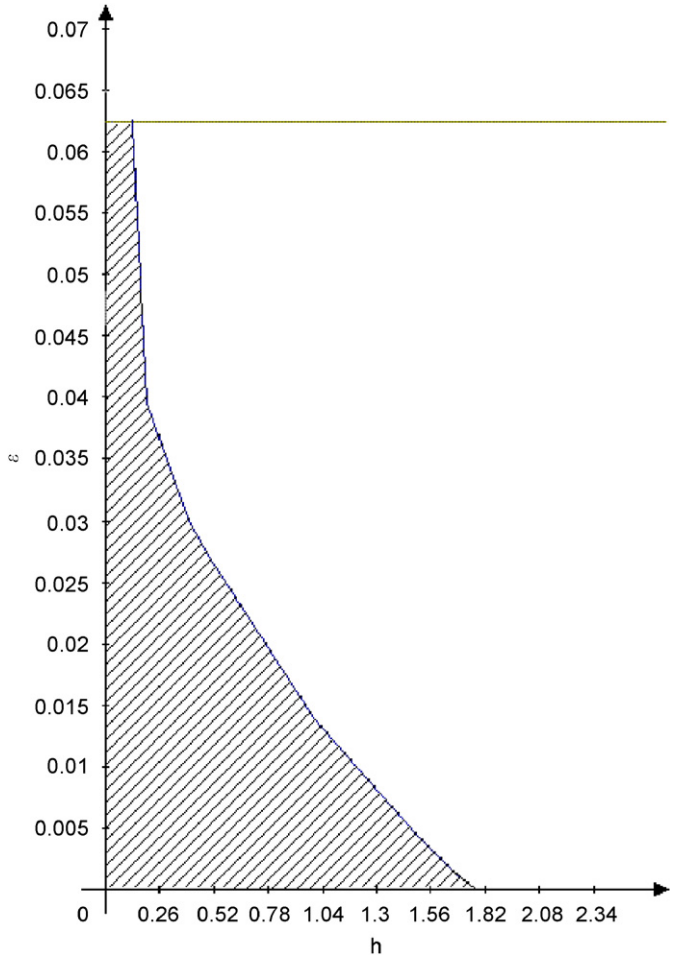

Fig. 6. The region of the unstable oscillations.

Now a stability of the second NNM (12) is analyzed. Then the system of the variational equation (31) has the following form:

$$\ddot{u} + u\tilde{\theta}_2^2 - \tfrac{1}{4}u + \varepsilon(u + 2vg(\tilde{\theta}_2)\tilde{\theta}_2) + O(\varepsilon^2) = 0, \tag{39a}$$

$$\ddot{v} + 12v\tilde{\theta}_2^2 - v + \varepsilon(16v + 2ug(\tilde{\theta}_2)\tilde{\theta}_2) + O(\varepsilon^2) = 0, \tag{39b}$$

where the function $\tilde{\theta}_2(\tau)$ is determined by Eq. (25).

A boundary between stable and unstable solutions, which corresponds to the periodic solutions of system (39) with a period $T = 2\pi\omega^{-1}$, is considered. Following the book [22], this boundary is presented as the Fourier series:

$$u = \sum_{i=0}^{\infty} U_{2i}\cos(2i\omega\tau), \quad v = \sum_{i=1}^{\infty} V_{2i-1}\cos((2i-1)\omega\tau). \tag{40}$$

Series (40) is substituted into Eq. (39) and the coefficients of the same harmonics are equated. As a result, the homogeneous system of linear algebraic equations is derived. The equation of the boundary between stable and unstable solutions has the following form:

$$\det(\mathbf{Z}) = 0, \tag{41}$$

where

$$\det(Z) = \det\begin{pmatrix} m_2 & 0.5c_1 & 0.25\theta_{2,\max}^2 & 0.5c_3 & 0 & 0.5c_5 \\ c_1 & -\omega^2 + m_1 & 0.5c_1 & 3\theta_{2,\max}^2 & 0.5c_3 & 0 \\ 0.5\theta_{2,\max}^2 & 0.5c_1 & -4\omega^2 + m_2 & 0.5c_1 & 0.25\theta_{2,\max}^2 & 0.5c_3 \\ c_3 & 3A^2 & 0.5c_1 & -9\omega^2 + m_1 & 0.5c_1 & 3\theta_{2,\max}^2 \\ 0 & 0.5c_3 & 0.25\theta_{2,\max}^2 & 0.5c_1 & -16\omega^2 + m_2 & 0.5c_1 \\ c_5 & 0 & 0.5c_3 & 3\theta_{2,\max}^2 & 0.5c_1 & -25\omega^2 + m_1 \end{pmatrix},$$

$$c_1 = \theta_{2,\max}^2\varepsilon(2b_0 + 1.5b_2\theta_{2,\max}^2 + 1.25b_4\theta_{2,\max}^4),$$

$$c_3 = \theta_{2,\max}^3\varepsilon\left(0.5b_2 + \tfrac{5}{8}b_4\theta_{2,\max}^2\right),$$

$$c_5 = \tfrac{5}{8}\varepsilon b_4\theta_{2,\max}^5,$$

$$m_1 = -1 + 6\theta_{2,\max}^2 + 16\varepsilon,$$

$$m_2 = -0.25 + 0.5\theta_{2,\max}^2 + \varepsilon.$$

Now the boundary between stable and unstable vibrations, which corresponds to the solutions of the period $2T$, is analyzed. The solutions of system (39) are presented by the Fourier series:

$$u = \sum_{i=1} U_{2i-1}\cos\left(\frac{2i-1}{2}\omega\tau\right),$$

$$v = \sum_{i=1} V_{2i-1}\cos\left(\frac{2i-1}{2}\omega\tau\right). \tag{42}$$

Making some algebra, which is similar to the previous analysis of the period T solutions, it is derived the following equation for the boundary between the stable and unstable solutions:

$$\det(\mathbf{Z}_2) = 0, \tag{43}$$

where

$$\det(\mathbf{Z}_2 =) = \det\begin{pmatrix} z_1 & -0.25\omega^2+m_1 & z_1 & 3A^2 & z_3 & 3A^2 \\ -0.25\omega^2+m_2 & z_1 & 0.25A^2 & z_1 & 0.25A^2 & z_3 \\ z_1 & 3A^2 & z_3 & -2.25\omega^2+m_1 & z_1 & 0 \\ 0.25A^2 & z_1 & -2.25\omega^2+m_2 & z_3 & 0 & z_1 \\ z_3 & 3A^2 & z_1 & 0 & z_5 & -6.25\omega^2+m_1 \\ 0.5A^2 & z_3 & 0 & z_1 & -6.25\omega^2+m_2 & z_5 \end{pmatrix},$$

$$z_1 = \varepsilon A\left(b_0 + 0.75b_2A^2 + \tfrac{5}{8}b_4A^4\right),$$

$$z_3 = \varepsilon A^3\left(0.25b_2 + \tfrac{5}{16}b_4A^2\right), \quad z_5 = \tfrac{1}{16}\varepsilon b_4A^5. \tag{44}$$

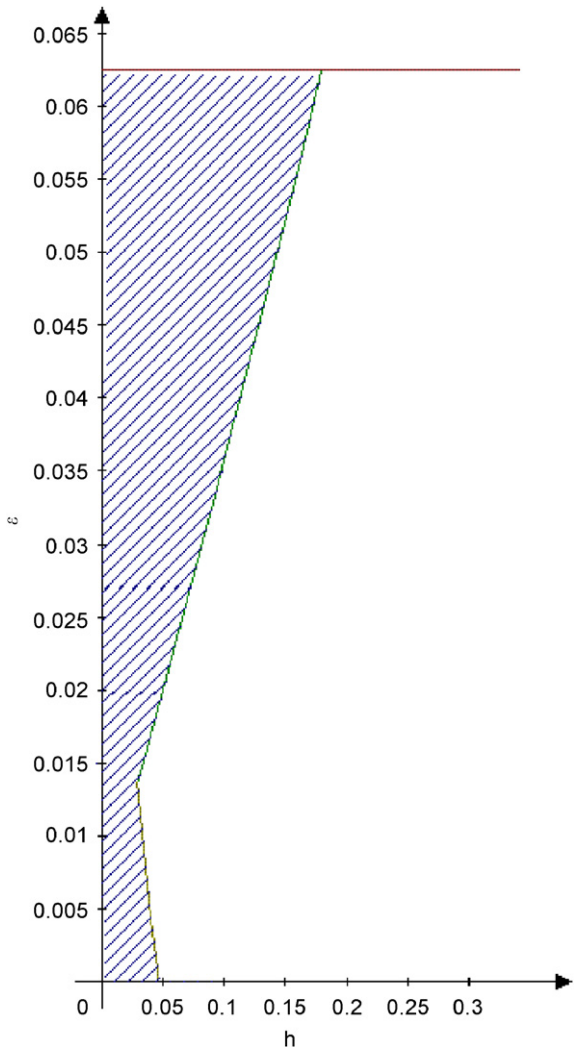

Fig. 7. The region of the unstable NNM (12).

Fig. 7 shows results of the numerical calculations of the boundary of the unstable trivial solutions of system (39) on the parametric plane (ε, h). These calculations are carried out according to Eqs. (43) and (44). The shaded region corresponds to the unstable NNM (12).

5. The direct numerical simulations of the snap-through motons

In order to analyze the dynamics of the shallow arch, the deflection $u(\tau, \xi)$ is expanded with respect to the beam modes (6). Moreover, only two modes are taken into account. In order to check this expansion, and the adequacy of the discrete model (8) to the partial differential equation (4), a direct numerical simulation of Eq. (4) is carried out.

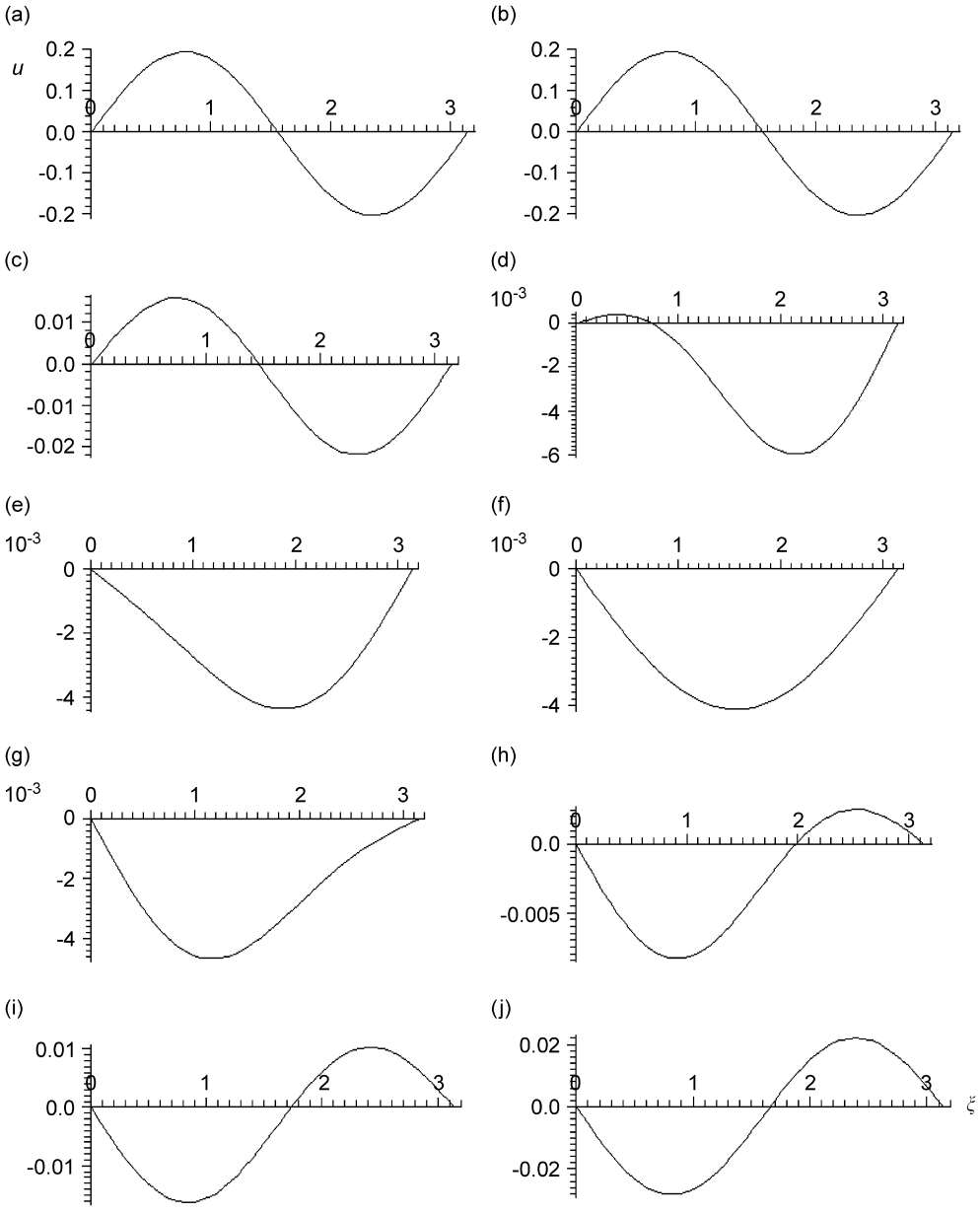

Fig. 8. The results of the direct numerical simulations.

Using the difference approximations [23], the partial differential equation (4) is replaced by the following system of ODE:

$$\frac{\mathrm{d}^2 u_i}{\mathrm{d}\tau^2} + \varepsilon\left[\frac{1}{h^4}(u_{i-2} - 4u_{i-1} + 6u_i - 4u_{i+1} + u_{i+2}) - \sin(\xi_i)\right] - \frac{1}{4\pi h}(u_{i-1} - 2u_i + u_{i+1}) \times \sum_{j=1}^{n+1}\left[\frac{1}{h^2}((u_{j-2} - u_{j-1})^2 + (u_{j-1} - u_j)^2) - (\cos^2(\xi_{j-1}) + \cos^2(\xi_j))\right] = 0, \tag{45}$$

where $i = \overrightarrow{1,n}$; n is the number of equations; $\xi_I = ih$. The solutions of Eq. (4) satisfy the boundary conditions, which takes the following form:

$$\begin{aligned} &u_0 = 0,\\ &u_{n+1} = 0,\\ &u_{-1} - 2u_0 + u_1 = 0,\\ &u_n - 2u_{n+1} + u_{n+2} = 0. \end{aligned} \tag{46}$$

The aim of this section is a modeling of the NNM (12) by solving system (46). We would like to confirm, that the motions, which are described by two terms of expansion (6) and (12), exist in system (4). Therefore, the initial conditions of system (45) are obtained from Eqs. (12), (23), and (24). The following initial conditions are used:

$$\begin{aligned} u_i(0) &= \theta_1 \sin(\xi_i) + \theta_2 \sin(2\xi_i),\\ \left.\frac{\mathrm{d}u_i}{\mathrm{d}\tau}\right|_{t=0} &= 0; i = \overrightarrow{1,n},\\ \theta_1 &= 0.024,\ \theta_2 = 1.263,\ \varepsilon = 0.02. \end{aligned} \tag{47}$$

In calculations the number of equations (46) is taken as $n = 51$. System (46) is solved by the Runge–Kutta method. The solutions of this system in the form of the flexure of the shallow arch at the different values of time are shown in Fig. 8. Fig. 8 verifies that the first and the second beam modes take part in the vibrations. Moreover, the second mode dominates. As follows from the calculations higher beam modes do not take part in these vibrations.

6. Conclusions

The snap-through motions of a shallow arch are investigated by means of nonlinear modes. These complex motions are analyzed only due to the use of Rosenberg nonlinear modes [17]. We stress, that very effective Shaw–Pierre nonlinear modes [24,25] exist, which allow one to study motions with many degree-of-freedom. However, using this approach, only the motions close to equilibria can be analyzed.

Two nonlinear modes are analyzed by the Rosenberg approach. One of these modes corresponds to symmetrical snap-through motions, when only the first spatial beam mode $\sin(\xi)$ takes part in the vibrations. The second nonlinear mode corresponds to more complex motions of the system, when nonsymmetrical snap-through motions take place. In this case, the first and the second spatial beam modes $\sin(\xi)$ and $\sin(2\xi)$ interact. Besides the nonlinear modes which have been analyzed complex motions can exist [17], which are not considered in this paper. These motions can be obtained by other analytical and numerical methods.

The backbone curves of the nonlinear modes are investigated and it is noted that the corresponding backbone curves for both the nonlinear modes are hard. These nonlinear modes are unstable for small amplitudes of vibration, when the dynamical system is close to a homoclinic orbit. Unstable motions are transformed into stable ones, when the dynamical system is distant from the homoclinic orbit.

The nonlinear modes, which are obtained analytically, are checked by means of direct numerical integration of the equations of motions. The results of the simulation show the vicinity of the analytical and numerical data.

The direct numerical integration of the nonlinear partial differential equations by means of the method of finite difference is used to check the two mode approximation of the snap-though motions of the shallow arch. The results indicate that the two mode approximation of motions is enough. Moreover, by means of the finite difference integration, we confirm the existence of nonlinear modes of the arch vibration.

Appendix A. The equation of bondary of dynamical instability

The boundary of the dynamical instability is determined from the equation:

$$\det(\mathbf{Q}) = 0,$$

where nonzero elements of the matrix Q are the following:

$$\begin{aligned}
q_{11} &= 0.5hk_1^2 - 0.5\varepsilon k_1k_2 + e_2k_2^2,\\
q_{21} &= -0.5\varepsilon k_1^2 - 0.5e_1k_1k_2 + 0.5\varepsilon k_3 - 2e_2k_1k_2,\\
q_{31} &= (0.25k_1^2 + 0.5k_3)e_1 - 1.5\varepsilon k_1 + k_2^2,\\
q_{41} &= -\tfrac{15}{8}k_1k_2 - 1.5k_1e_1 + k_2^2,\\
q_{51} &= -\tfrac{1}{32}k_1^2 + \tfrac{7}{8}k_3 + e_1 + e_2,\\
q_{61} &= -\tfrac{13}{8}k_1,\\
q_{11} &= 0.5hk_1^2 - 0.5\varepsilon k_1k_2 + e_2k_2^2,\\
q_{12} &= -2hk_1k_2 + \varepsilon k_2^2,\\
q_{22} &= 0.5hk_1^2 + 2hk_3 + k_2^2e_1 - 0.5\varepsilon k_1k_2 + k_2^2e_2,\\
q_{32} &= -3.5k_1k_2e_1 - 0.5\varepsilon k_3 - 0.5\varepsilon k_1^2 - 6hk_1 - 2k_1k_2e_2,\\
q_{42} &= (0.25k_1^2 + 2.5k_3)e_1 - 2.5\varepsilon k_1 + 4h + 0.75k_2^2 + k_3e_2,\\
q_{52} &= -1.25k_1k_2 - 6.5e_1 - 2\varepsilon - 2k_1e_2,\\
q_{62} &= -\tfrac{1}{32}k_1^2 + 0.5k_3 + 3e_1 + e_2,\\
q_{13} &= 4hk_2^2,\\
q_{23} &= -2\varepsilon k_2^2 - 12k_1k_2,\\
q_{33} &= 4k_2^2e_1 + 7.5\varepsilon k_1k_2 + 2h(0.25k_1^2 + 4k_3) + k_2^2e_2,\\
q_{43} &= -10.5k_1k_2e_1 - 0.5\varepsilon k_1^2 - 5.5\varepsilon k_3 - 20hk_1 - k_1k_2e_2,\\
q_{53} &= 0.25k_2^2 + (0.25k_1^2 + 6.5k_3 + 2k_2^2)e_1 + 14.5\varepsilon k_1 + 12h + k_3e_2,\\
q_{63} &= -\tfrac{1}{8}k_1k_2 - 15.5k_1e_1 - 9\varepsilon - 2k_1e_2,\\
q_{14} &= 0,\\
q_{24} &= 12hk_2^2,\\
q_{34} &= -9\varepsilon k_2^2 - 30hk_1k_2,\\
q_{44} &= 9k_2^2e_1 + 23.5\varepsilon k_1k_2 + 2h(0.25k_1^2 + 9k_3) + k_2^2e_2,\\
q_{54} &= -21.5k_1k_2e_1 - 14.5\varepsilon k_3 - 0.5\varepsilon k_1^2 - 42hk_1 - 2k_1k_2e_2,\\
q_{64} &= -0.5k_2^2 + (0.25k_1^2 + 12.5k_3)e_1 + 34.5\varepsilon k_1 + 24h - \tfrac{1}{8}k_3 + k_3e_2,
\end{aligned}$$

$$q_{15} = 0,$$
$$q_{25} = 0,$$
$$q_{35} = 24hk_2^2,$$
$$q_{45} = -20\varepsilon k_2^2 - 56hk_1k_2,$$

$$q_{55} = 47.5\varepsilon k_1k_2 + 2h(0.25k_1^2 + 16k_3) + 4k_2^2e_1 + k_2^2e_2,$$
$$q_{65} = -36.5k_1k_2e_1 - 27.5\varepsilon k_3 - 0.5\varepsilon k_1^2 - 72hk_1 - k_1k_2e_2,$$
$$q_{16} = 0,$$
$$q_{26} = 0,$$

$$q_{36} = 0,$$
$$q_{46} = 40hk_2^2,$$
$$q_{56} = -35\varepsilon k_2^2 - 90hk_1k_2,$$
$$q_{66} = 25k_2^2e_1 + 2h(0.25k_1^2 + 25k_3) + 79.5\varepsilon k_1k_2 + k_2^2e_2,$$

$$k_1 = X_1 + X_2,$$
$$k_2 = X_1X_2,$$
$$k_3 = X_1^2 + 4X_1X_2 + X_2^2,$$
$$e_1 = 0.25 - \varepsilon,$$
$$e_2 = 16\varepsilon - 1.$$

References

[1] L.N. Virgin, R.B. Davis, Vibration isolation using buckled struts, *Journal of Sound and Vibration* 260 (2003) 965–973.
[2] K.V. Avramov, Yu.V. Mikhlin, Snap-through truss as a vibration absorber, *Journal of Vibration and Control* 10 (2004) 291–308.
[3] K.V. Avramov, Yu.V. Mikhlin, Snap-through truss as an absorber of forced oscillations, *Journal of Sound and Vibration* 29 (2006) 705–722.
[4] V.A. Budginskii, On the use of the snap-through membrane for limitation of dynamical loads, *Mechanics of Solids* 4 (1989) 44–49.
[5] S.P. Timoshenko, Buckling of flat curved bars and slightly curved plates, *ASME Journal of Applied Mechanics* 2 (1935) 17–20.
[6] A.N. Dinnik, *Stability of Arches*, Gostehizdat, Moscow, 1946 (in Russian).
[7] Ed. Grigoluk, On the calculations of stability of shallow arches, *Ingenernij Sbornik* 9 (1951) 177–200 (in Russian).
[8] Y.C. Fung, A. Kaplan, Buckling of low arches or curved beams of small curvature, NACA Technical Note 2840, 1952.
[9] C.S. Hsu, Stability of shallow arches against snap-through under timewise step loads, *ASME Journal of Applied Mechanics* 33 (1968) 31–39.
[10] C.S. Hsu, C.T. Kuo, R.H. Plant, Dynamic stability criteria for clamped shallow arches under timewise step loads, *AIAA Journal* 7 (1969) 1925–1931.
[11] N.C. Hung, Dynamic buckling of some elastic shallow structures subjected to periodic loading with high frequency, *International Journal of Solids and Structures* 8 (1972) 315–326.
[12] L.I. Manevich, Y.V. Mikhlin, V.N. Pilipchuk, *Method of Normal Vibrations for Essential Nonlinear Systems*, Nauka, Moscow, 1989 (in Russian).
[13] S. Lenci, N. Tarantino, Dynamics of shallow elastic arches. Part 1: chaotic response of harmonically shaped arches, *European Journal of Mechanics, A/Solids* 3 (1996) 513–528.
[14] J.-S. Lin, J.-S. Chen, Dynamic snap-through of a laterally loaded arch under prescribed end motion, *International Journal of Solids and Structures* 40 (2003) 4769–4787.
[15] J.-S. Chen, C.-Y. Liao, Experiment and analysis on the free dynamics of a shallow arch after an impact load at the end, *ASME Journal of Applied Mechanics* 72 (2005) 54–61.
[16] J.-S. Chen, J.-S. Lin, Dynamic snap-through of a shallow arch under a moving point load, *ASME Journal of Vibration and Acoustics* 126 (2004) 514–519.
[17] A. Vakakis, L.I. Manevich, Y.V. Mikhlin, V.N. Pilipchuk, A.A. Zevin, *Normal Modes and Localization in Nonlinear Systems*, Wiley Interscience, New York, 1996.
[18] E.L. Ince, *Ordinary Differential Equations*, Longmans Green, London, 1926.

[19] Yu.V. Mikhlin, A.L. Zhupiev, An application of the Ince algebraization to the stability of nonlinear normal vibration modes, *International Journal of Nonlinear Mechanics* 32 (1997) 493–509.
[20] Y.V. Mikhlin, S.N. Reshetnikova, Dynamical interaction of an elastic system and essential nonlinear absorber, *Journal of Sound and Vibration* 283 (2005) 91–120.
[21] T.S. Parker, L.O. Chua, *Practical Numerical Algorithms for Chaotic Systems*, Springer, New York, 1989.
[22] V.V. Bolotin, *The Dynamic Stability of Elastic Systems*, Holden-Day, San Francisco, 1964.
[23] S. Foale, J.M.T. Thompson, F.A. McRobie, Numerical dimension-reduction methods for non-linear shell vibrations, *Journal of Sound and Vibration* 215 (3) (1998) 527–545.
[24] S.W. Shaw, C. Pierre, Normal modes for nonlinear vibratory systems, *Journal of Sound and Vibrations* 164 (1993) 58–124.
[25] K.V. Avramov, C. Pierre, N. Shiraeva, Flexural- flexural–torsional nonlinear vibrations of pre-twisted rotating beams with asymmetrical cross section, *Journal of Vibration and Control* 13 (2007) 329–365.